A Novel Flux Linkage Measurement Method for Linear Switched Reluctance Motors

Shi Wei Zhao, *Member, IEEE*, Norbert C. Cheung, *Senior Member, IEEE*, Wai-Chuen Gan, *Senior Member, IEEE*, and Zhen Gang Sun, *Student Member, IEEE*

***Abstract*—The magnetic characteristics of a linear switched reluctance motor (LSRM) are important in its performance prediction and verification. Owing to the complicated magnetic paths, the measurement of the flux linkage for this type motor has drawn many researchers' attentions. In this paper, a new flux linkage measurement method for LSRMs is proposed to obtain the flux linkage characteristics of LSRMs using an online winding resistance estimation technique. Both the theoretical derivation and the actual implementation of the proposed method are addressed in this paper. In comparison with the search coil scheme and the static resistor scheme, experimental results confirm the validity and accuracy of this method. In short, the proposed method is simple, effective, and easy to be implemented. It is a practical solution for flux linkage measurement of LSRMs and other motors.**

***Index Terms*—Error analysis, flux linkage measurement, linear switched reluctance motor (LSRM), online resistor estimation, switched reluctance motor (SRM).**

I. Introduction

In RECENT years, switched reluctance motors (SRMs) have received considerable attention for industrial applications due to their low cost, simple structures, ruggedness, and reliability in harsh environments and the capability of a wide speed range [1], [2]. In addition to these advantages, linear SRMs (LSRMs) can reduce the space requirement for their installation because there is no extra mechanical component to product linear motion, such as couplers and ball screws. These reasons also make LSRM as an alternative choice for direct-drive applications [3], [4].

The electromagnetic force generation of SRMs and LSRMs is related to the flux linkage of phase windings. Because of the doubly salient structure, the magnetic circuit of SRMs is complicated and hard to predict its performances using traditional methods. The finite-element method (FEM) [5], [6] can be used to study the flux linkage of LSRMs and perform optimization on motor design. However, the accuracy of the results heavily depends on the skill of the user in choosing the mesh elements and the availability of the magnetic characteristic data of the different materials used. In addition, the method is computational complex and time consuming. Generally, actual measurement is easier to perform for design verification and more direct to provide data for flux linkage modeling.

Existing measurement methods of the flux linkage can be grouped into direct and indirect methods. Direct measurement of the flux linkage is to employ magnetic sensors to measure flux linkage inside the motor [7]. This method is seldom used due to the inconvenience and high cost. On the other hand, indirect methods [8]–[16] are more popular in that they are simple, low cost, and easy to implement. Again, these methods can be grouped as search coil methods [8], [9] and step voltage methods [10]–[16].

For a step voltage scheme, a step voltage energizes a phase winding, and the flux linkage in this phase winding is calculated using the phase voltage and current values. This measurement scheme can be implemented using either an analog integrator [10], [11] or a digital integrator [12]–[16]. For this method, the measurement accuracy is dependent on the winding resistor value, which may vary with the test conditions such as the circumstance temperature, current level, etc. To ensure good accuracy, special methods are employed, such as matching an exact power resistor [11] and online measurement of the winding resistance [16], where the winding resistance is calculated by using the steady current.

For a search coil scheme [8], [9], a search coil is placed in a phase winding, which is excited by an ac voltage source. The flux linkage in this phase winding is calculated by integrating the induced electromotive force (EMF) developed at the search coil. This method avoids the resistor value-changing problem and can provide relative good measurement accuracy. However, the installation of search coils is often cumbersome and sometimes even impossible.

In this paper, a new method for flux linkage measurement is proposed, and the winding resistor is estimated with online fashion. By feeding an ac voltage to a phase winding, the flux linkage is calculated using the phase voltage and current data. This method is simple, effective, and easy to be implemented. In comparison with the search coil method, experiment results demonstrate that this method can achieve good measurement accuracy.

The organization of this paper is as follows: Construction of the LSRM and the proposed method are given in Section II.

Manuscript received February 27, 2008; revised April 28, 2008. Current version published September 16, 2009. This work was supported by the University Grants Council through Projects PolyU 5224/04E and PolyU 5141/05E. The Associate Editor coordinating the review process for this paper was Dr. Subhas Mukhopadhyay.

S. W. Zhao, N. C. Cheung, and Z. G. Sun are with the Department of Electrical Engineering, Hong Kong Polytechnic University, Kowloon, Hong Kong (e-mail: eencheun@inet.polyu.edu.hk).

W.-C. Gan is with ASM Assembly Automation Hong Kong Ltd., Kwai Chung, Hong Kong.

Color versions of one or more of the figures in this paper are available online at http://ieeexplore.ieee.org.

Digital Object Identifier 10.1109/TIM.2009.2018683

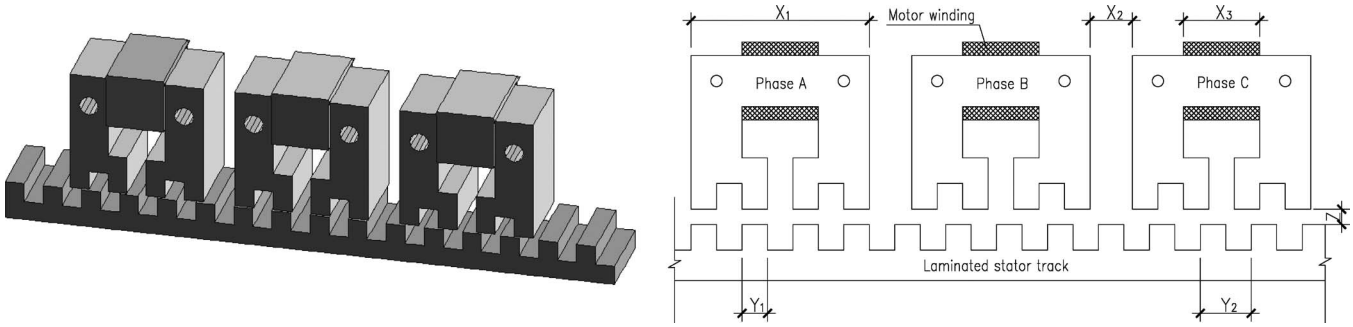

Fig. 1. Schematic of the LSRM.

Error analysis is presented in Section III. The experimental setup and result analysis are stated in Sections IV and V, respectively. Concluding remarks are made in Section VI.

II. Proposed Method

A. Construction of the LSRM

The proposed LSRM is a three-phase motor, and its design schematic is shown in Fig. 1. This LSRM comprise two components, which are known as the moving platform and the stator track. A set of three-phase coils with the same dimensions is installed on the moving platform. The three phase windings are separated by 120 electrical degrees from each other. The body of the moving platform is manufactured with aluminum, so that the total weight of the moving platform is low and the magnetic paths are decoupled. The moving platform is mounted on two slider blocks, which are tightly fixed on the bottom of the LSRM. This rugged mechanical structure can effectively buffer extended vibration during its operation. The stator track is fixed on the base of the LSRM. Both the stator track and the core of the windings are laminated with 0.5-mm silicon-steel plates. The electrical and mechanical parameters are listed in Table I.

For the LSRM, any one of the three phases on the moving platform is referred to be the aligned position, where its teeth fully correspond to any teeth on the stator track. In this position, the phase reluctance has the minimum value. A phase position is referred to be the unaligned position, where the teeth of the phase fully correspond to the slots of the stator track, and the phase reluctance achieves its maximum value there (Table I).

TABLE I
Mechanical and Electrical Parameters of the LSRM

Max travel distance	300mm
Motor length (x_1)	146mm
Phase separation (x_2)	10mm
Pole width (y_1)	6mm
Pole pitch (y_2)	12mm
Wind length	18mm
Wind width	25mm
Air gap width (z)	0.5mm
Mass of the moving platform	1.8Kg
Phase resistance	1.5Ω
Aligned inductance	10.2mH
Unaligned inductance	7.8mH

B. Mathematical Model and Measurement Principle

For an LSRM, the voltage equation of a phase winding is given as

$$v = ri + \frac{d\lambda}{dt} \tag{1}$$

where v, i, r, and λ denote the terminal voltage, winding current, winding resistance, and winding flux linkage, respectively. The second term on the right-hand side of (1) is referred to as the EMF. For a fixed position, the winding flux linkage is a function of the winding inductance L and current. Because of the saturation effect, the winding inductance is also a function of the winding current. Therefore, (1) can further be rearranged as

$$v = ri + L\frac{di}{dt} + i\frac{dL}{di}\frac{di}{dt}. \tag{2}$$

Under an ac voltage excitation, two assumptions for the produced winding current can be posed.

1) The winding current is a periodic signal.
2) The winding current is continuous and differentiable.

These two assumptions can be verified from observing experimental results. When a periodic voltage source is applied to a phase winding, it is reasonable that a periodic winding current is produced, although it may contain harmonics. As an inductance, the current in a phase winding is prone to continuously change for a continuous voltage excitation.

For the online estimation of the winding resistor value, extreme points of the winding current in each period could be observed. The differential of the winding current along time in these extreme points would be zero. Take a maximum point $i(T)$ as an example. In this period, the winding current increases before it attains the maximum point; hence, the differential of the winding current along time is positive, as shown in (3). However, the current decreases after it attains the maximum point; hence, the differential becomes negative, as shown in (4). Furthermore, (5) should hold for ensuring continuous

and differentiable winding current. Hence, the differential of the winding current in the maximum point should be zero, as shown in (6). The aforementioned equations are given as follows:

$$\frac{di(t)}{dt} > 0, \qquad t < T. \tag{3}$$

$$\frac{di(t)}{dt} < 0, \qquad t > T. \tag{4}$$

$$\lim_{t \to T-} \frac{di(t)}{dt} = \lim_{t \to T+} \frac{di(t)}{dt}. \tag{5}$$

$$\left.\frac{di(t)}{dt}\right|_{t=T} = 0. \tag{6}$$

By substituting (6) into (2), it can be found that the whole terminal voltage is loaded across the winding resistor and that there is no voltage in the winding inductance. Therefore, the winding resistance at this time can be represented by

$$r(T) = \frac{v(T)}{i(T)}. \tag{7}$$

which is also valid for minimum points.

As the excitation period is rather short, the estimated winding resistance could be treated as the resistor value in the following period. This way, the estimated resistance can be used to calculate flux linkage online and be updated in each period. Therefore, the winding flux linkage can be represented as

$$\lambda(t) = \int_0^t (v(\tau) - r(\tau) i(\tau))\, d\tau + \lambda(0) \tag{8}$$

where $\lambda(0)$ denotes the flux linkage at time $t = 0$. By calculating the initial value before the integration, it can be eliminated by an offset removal program.

Finally, the EMF on the phase winding e can be represented as

$$e(t) = v(t) - r(t) i(t). \tag{9}$$

III. Error Analysis

The measurement error of the flux linkage is investigated from the measurement error of the terminal voltage, the measurement error of the winding current, and the estimation error of the winding resistor, in that the three error sources are directly related to the flux linkage, as shown in (8).

The measurement error of the terminal voltage, the measurement error of the winding current, and the estimation error of the winding resistor are denoted by Δv, Δi, and Δr, respectively, which are defined as follows:

$$v_{\mathrm{mea}} = v + \Delta v \tag{10}$$

$$i_{\mathrm{mea}} = i + \Delta i \tag{11}$$

$$r_{\mathrm{est}} = r + \Delta r \tag{12}$$

where v_{mea}, i_{mea}, and r_{est} denote the measured terminal voltage, the measured winding current, and the estimated winding resistance, respectively. The measured winding flux linkage λ_{mea} and the estimated EMF e_{est} can be expressed as

$$\lambda_{\mathrm{mea}}(t) = \int_0^t (v_{\mathrm{mea}}(\tau) - r_{\mathrm{est}}(\tau) i_{\mathrm{mea}}(\tau))\, d\tau. \tag{13}$$

$$e_{\mathrm{est}}(t) = v_{\mathrm{mea}}(t) - r_{\mathrm{est}}(t) i_{\mathrm{mea}}(t). \tag{14}$$

The measurement error of the flux linkage can be obtained by comparing the theoretical representation (8) with the measured representation (13). Therefore, the measurement error of the flux linkage $\Delta\lambda$ can be expressed as

$$\Delta\lambda(t) = \int_0^t (\Delta v(\tau) - \Delta r(\tau)\Delta i(\tau) - \Delta r(\tau) i(\tau) - \Delta i(\tau) r(\tau))\, d\tau. \tag{15}$$

In addition, the estimation error of the EMF Δe can be expressed as

$$\Delta e(t) = \Delta v(t) - \Delta r(t)\Delta i(t) - \Delta r(t) i(t) - \Delta i(t) r(t). \tag{16}$$

The measurement error of the flux linkage is the integration of the estimated EMF error. It can be seen that the estimation accuracy of the EMF depends on the measurement error of the terminal voltage, the measurement error of the winding current, and the estimation error of the winding resistor. As shown in the third term on the right-hand side of (16), the estimation error would further be enlarged with the winding current when the winding resistance is inaccurate. Apart from choosing precise current and voltage sensors, the estimation of the winding resistance is essential to ensure good overall accuracy.

IV. Experimental Configuration and Implementation

The flux linkage measurement system is composed of an LSRM with an encoder, a mechanical clamp, an ac voltage excitation source, a measurement board, and a digital acquisition system, as shown in Fig. 2. To provide comparison data, a search coil is placed over the measured phase winding. The mover of the LSRM is fixed to a particular position by the clamp. A 2-kW autotransformer is applied to provide a 50-Hz ac voltage excitation. The terminal voltage and winding current are measured by two Hall Effect sensors. The two signals and induced EMF from the search coil are inputted into the measurement board to be amplified and filtered. These signals, together with position information from the encoder, are collected by the digital acquisition system of the dSPACE card. The flux linkage and winding resistance are calculated online in the dSPACE digital acquisition system. The measured data are sampled at a frequency of 2 kHz, and the analog signals are fed into three 16-bit analog-to-digital converter channels.

To measure the flux linkage of the phase winding, a procedure is followed.

1) Calibrate the coefficients and offsets of the sensors and measurement circuit.

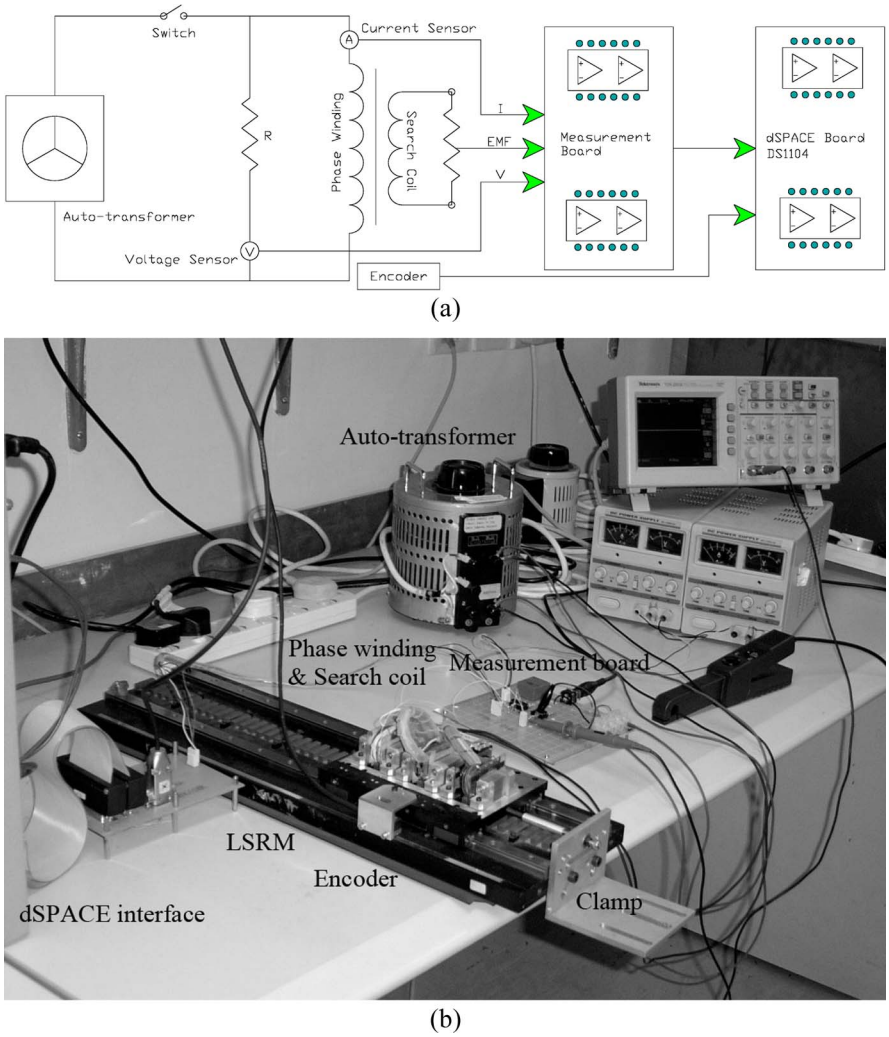

Fig. 2. Experimental setup for ac excitation flux linkage measurement of the LSRM. (a) Block diagram for the measurement scheme. (b) Photo of the actual installation.

2) Adjust the position of the LSRM's mover.
3) Adjust the autotransformer so that the desired maximum current is reached.
4) Switch on the autotransformer to excite the measured phase winding for a very short duration. Simultaneously, capture and store the terminal voltage, winding current, and induced EMF and calculate the flux linkage online.
5) Repeat steps 3 and 4 for different current levels.
6) Repeat steps 2–5 at different positions.

V. Experimental Results

Several experimental results are presented in this section. In the test, three schemes for the measurement of the flux linkage and EMF are compared, including the search coil scheme, the proposed scheme of online resistor estimation, and the static resistor scheme. For the static resistor scheme, the winding resistance is measured offline.

Figs. 3–5 show the waveforms of the terminal voltage, winding current, and induced EMF from the search coil when an ac excitation voltage is applied to the measured phase winding at the aligned position. The winding current and induced EMF

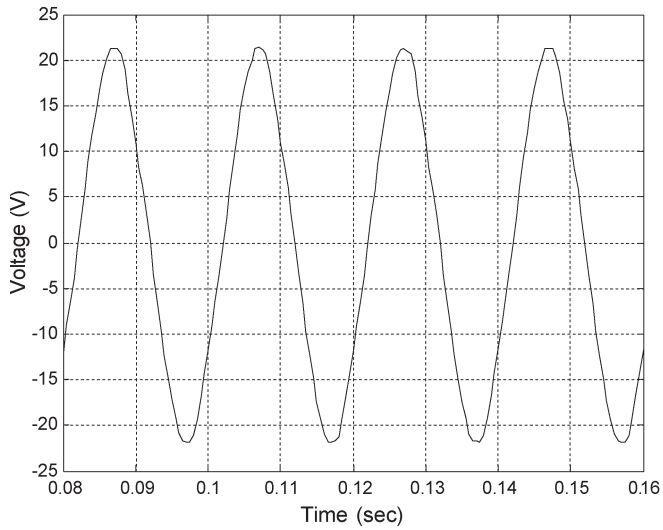

Fig. 3. Terminal voltage measured from the phase winding.

profiles are continuous and periodic signals, although both of them are nonsinusoidal. This is consistent with the assumptions mentioned earlier in this paper. Furthermore, it can be observed

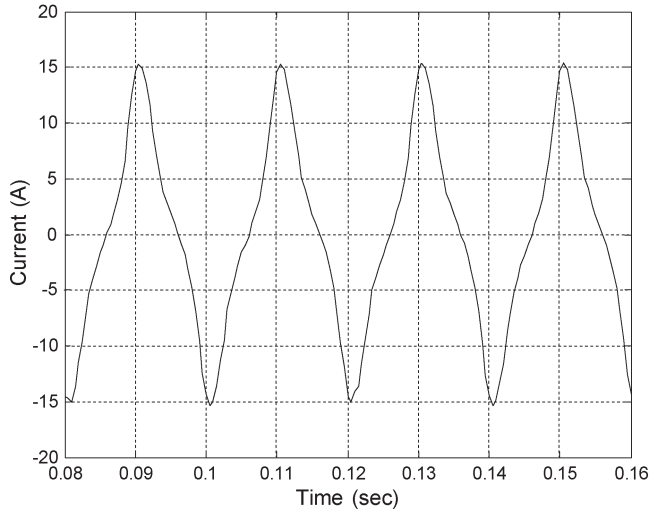

Fig. 4. Current profile of the measured phase winding.

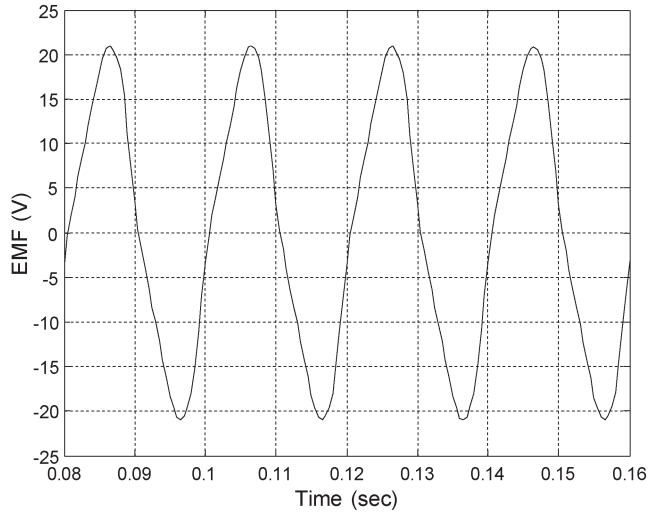

Fig. 5. Induced EMF waveform from the search coil.

that the EMF is almost zero when the winding current attains its extreme points. Again, this is consistent with the theoretical derivative result of the algorithm of online resistor estimation.

Fig. 6 shows the profile of the online estimated winding resistance. Different from the static resistor measured offline, the value of the online estimated resistor is updated in each period, as previously mentioned in this paper.

Fig. 7 shows the comparison of the EMF waveforms obtained by the three measurement schemes. The EMF waveform of the proposed scheme matches that of the search coil scheme very well, but the results of the static resistor scheme are a slightly different from those of the other two waveforms. Fig. 8 plots the EMF error profiles between the search coil scheme, the proposed scheme, and the static scheme. It can be found that the maximum EMF error between the search coil scheme and the static scheme is almost five times of that between the search coil scheme and the proposed scheme. This error profile shows that the proposed scheme can obtain a good EMF estimation, as compared with that measured from the search coil scheme.

Fig. 9 shows the comparison of the flux linkage waveforms obtained by the three measurement schemes. The flux linkage

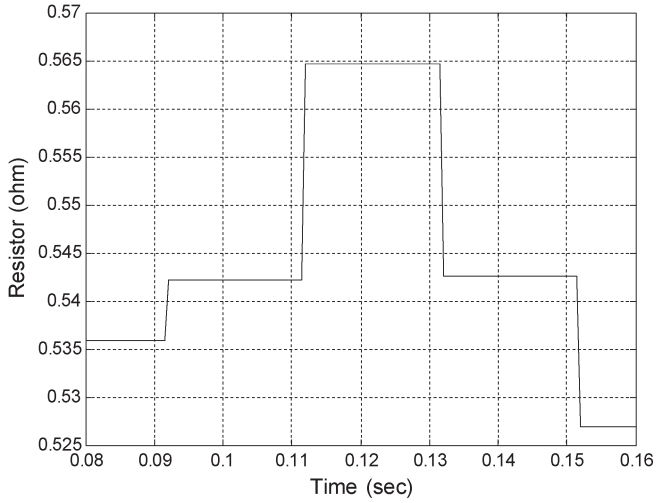

Fig. 6. Online estimated winding resistance profile.

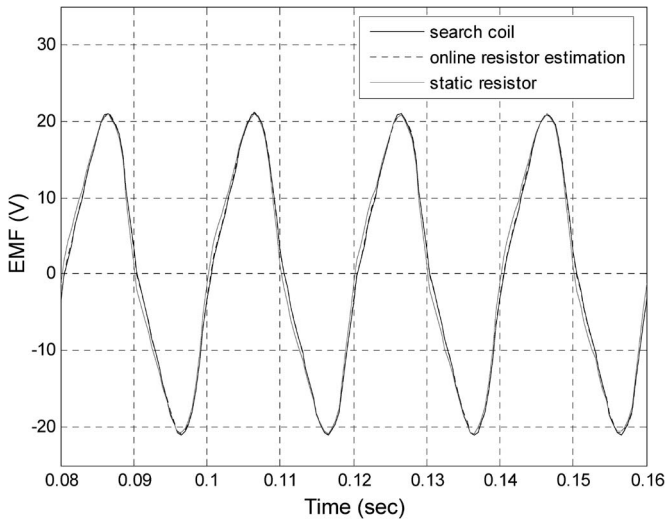

Fig. 7. Comparison of the EMF waveforms among the search coil method, the online resistor estimation method, and the static resistor method.

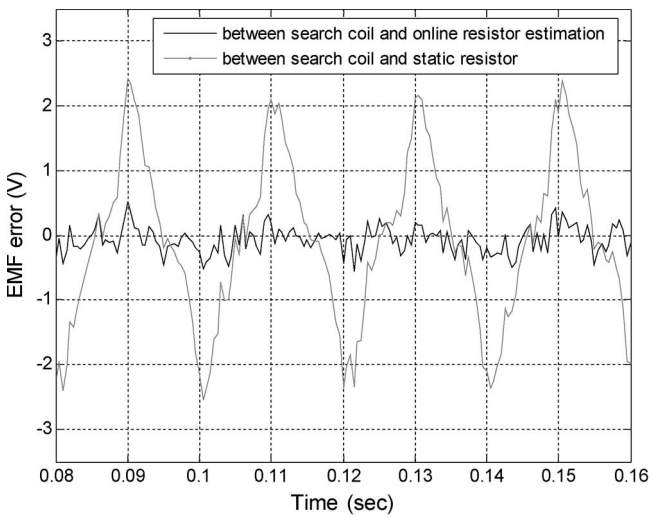

Fig. 8. EMF error profiles between the search coil method and the online resistor estimation method and between the search coil method and the static resistor method.

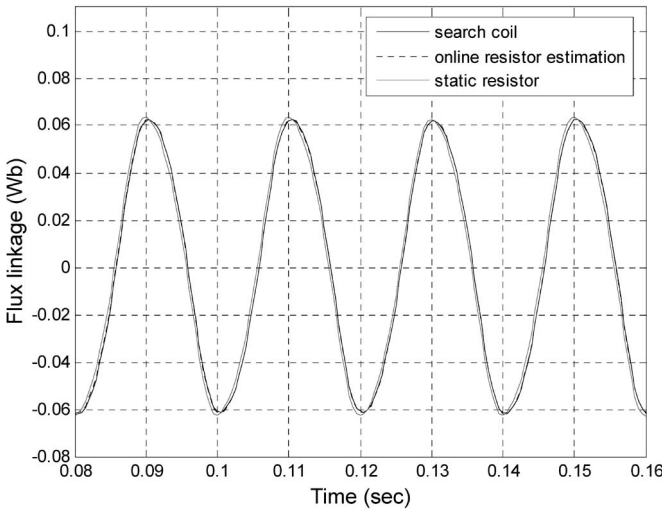

Fig. 9. Comparison of the flux linkage waveforms among the search coil method, the online resistor estimation method, and the static resistor method.

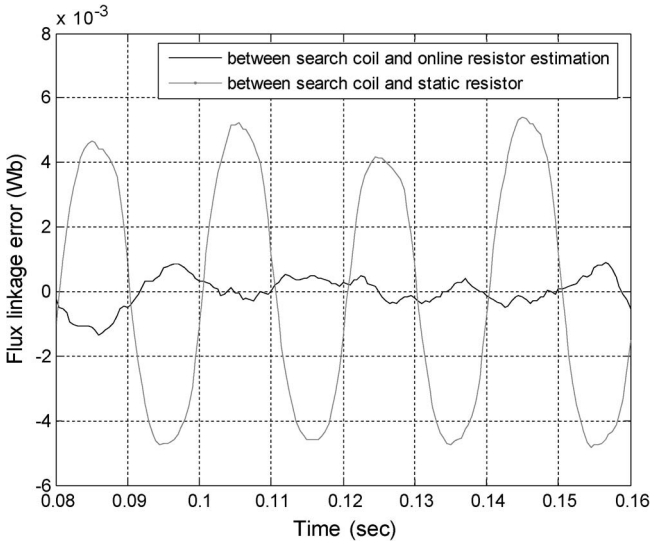

Fig. 10. Flux linkage error profiles between the search coil method and the online resistor estimation method and between the search coil method and the static resistor method.

waveform of the proposed scheme matches that of the search coil scheme well, but the results of the static resistor scheme are different from those of the other two waveforms. Fig. 10 plots the flux linkage errors between the search coil scheme, the proposed scheme, and the static scheme. The maximum flux linkage error between the search coil scheme and the proposed scheme is below 1.5 mWb, whereas the maximum flux linkage error between the search coil scheme and the static scheme is above 5 mWb. The latter is more than three times of the former.

Fig. 11 illustrates the hysteresis loops constructed by using the data from the three measurement schemes. It can be seen that the hysteresis loop of the proposed scheme is almost superposed with that of the search coil scheme, whereas the hysteresis loop is clearly bigger than the other two loops. It agrees with the contrastive results of the EMF and flux linkage, as shown in Figs. 7 and 9.

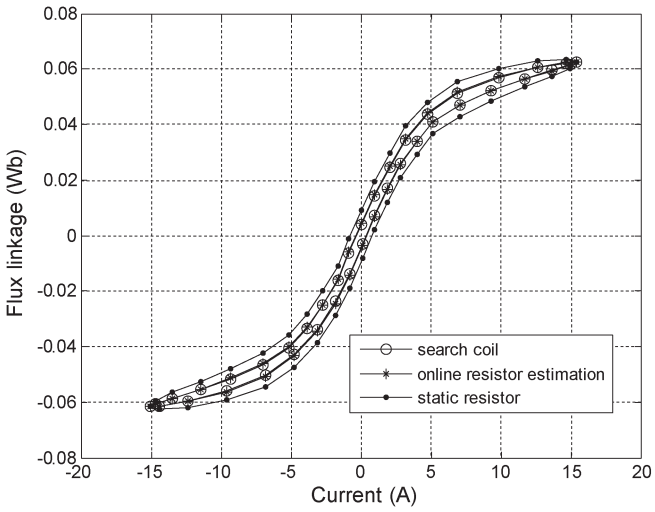

Fig. 11. Hysteresis loops by using the search-coil-based scheme, the proposed online resistor estimation scheme, and the static resistor scheme.

VI. Conclusion

In this paper, a new measurement method for flux linkage has been proposed. By using an online estimation technique of the winding resistor value, the flux linkage characteristics of the LSRM have been obtained. Both the theoretical derivation and the actual implementation of the proposed method have been addressed, respectively.

In comparison with the search coil scheme and the static resistor scheme, experimental results confirm the validity of this method and demonstrate the accuracy in practical measurements. The proposed method is simple, effective, and easy to be implemented. It is also a practical solution for flux linkage measurement of LSRMs and other motors.

References

[1] P. J. Lawrenson, J. M. Stephenson, P. T. Blenkinsop, J. Corda, and N. N. Fulton, "Variable-speed switched reluctance motors," *Proc. Inst. Elect. Eng.—Elect. Power Appl.*, vol. 127, no. 4, pt. B, pp. 253–265, Jul. 1980.

[2] M. Ilic'-Spong, R. Marino, S. M. Peresada, and D. G. Taylor, "Feedback linearizing control of switched reluctance motors," *IEEE Trans. Autom. Control*, vol. AC-32, no. 5, pp. 371–379, May 1987.

[3] H. S. Lim and R. Krishnan, "Ropeless elevator with linear switched reluctance motor drive actuation systems," *IEEE Trans. Ind. Electron.*, vol. 54, no. 4, pp. 2209–2218, Aug. 2007.

[4] S. W. Zhao, N. C. Cheung, W.-C. Gan, J. M. Yang, and J. F. Pan, "A self-tuning regulator for the high-precision position control of a linear switched reluctance motor," *IEEE Trans. Ind. Electron.*, vol. 54, no. 5, pp. 2425–2434, Oct. 2007.

[5] R. Arumugam, D. A. Lowther, R. Krishnan, and J. F. Lindsay, "Magnetic field analysis of a switched reluctance motor using a two dimensional finite element model," *IEEE Trans. Magn.*, vol. MAG-21, no. 5, pp. 1883–1885, Sep. 1985.

[6] S.-H. Mao and M.-C. Tsai, "A novel switched reluctance motor with C-core stators," *IEEE Trans. Magn.*, vol. 41, no. 12, pp. 4413–4420, Dec. 2005.

[7] J. C. Prescott and A. K. El-Kharashi, "A method of measuring self-inductances applicable to large electrical machines," *Proc. Inst. Elect. Eng.—Part A*, vol. 106, no. 26, pp. 169–173, Apr. 1959.

[8] A. Ferrero and A. Raciti, "A digital method for the determination of the magnetic characteristic of variable reluctance motors," *IEEE Trans. Instrum. Meas.*, vol. 39, no. 4, pp. 604–608, Aug. 1990.

[9] A. Ferrero, A. Raciti, and C. Urzi, "An indirect test method for the characterization of variable reluctance motors," *IEEE Trans. Instrum. Meas.*, vol. 42, no. 6, pp. 1020–1025, Dec. 1993.

[10] R. Krishnan and P. Materu, "Measurement and instrumentation of a switched reluctance motor," in *Conf. Rec. IEEE IAS Annu. Meeting*, 1989, vol. 1, pp. 116–121.
[11] W. F. Ray and F. Erfan, "A new method of flux or inductance measurement for switched reluctance motors," in *5th Int. Conf. Power Electron. Variable-Speed Drives*, 1994, pp. 137–140.
[12] V. K. Sharma, S. S. Murthy, and B. Singh, "An improved method for the determination of saturation characteristics of switched reluctance motors," *IEEE Trans. Instrum. Meas.*, vol. 48, no. 5, pp. 995–1000, Oct. 1999.
[13] V. K. Sharma, S. S. Murthy, and B. Singh, "An improved method for the determination of saturation characteristics of switched reluctance motors," *IEEE Trans. Instrum. Meas.*, vol. 48, no. 5, pp. 995–1000, Oct. 1999.
[14] S. C. Wang, W. S. Chen, W. B. Liao, K. Y. Shen, and Y. L. Chen, "A PC-based measurement system for determining magnetic characteristics of switched reluctance motors," in *Int. Conf. Power Syst. Technol.*, 2002, vol. 4, pp. 2256–2260.
[15] A. D. Cheok and N. Ertugrul, "Computer-based automated test measurement system for determining magnetization characteristics of switched reluctance motors," *IEEE Trans. Instrum. Meas.*, vol. 50, no. 3, pp. 690–696, Jun. 2001.
[16] A. D. Cheok and Z. Wang, "DSP-based automated error-reducing flux-linkage-measurement method for switched reluctance motors," *IEEE Trans. Instrum. Meas.*, vol. 56, no. 6, pp. 2245–2253, Dec. 2007.

Shi Wei Zhao (S'07–M'09) received the B.Sc. degree from Central South University, Changsha, China, in 2000 and the M.Sc. degree from South China University of Technology, Guangzhou, China, in 2003. He is currently working toward the Ph.D. degree at the Department of Electrical Engineering, Hong Kong Polytechnic University, Kowloon, Hong Kong.

His main research interests include motion control and machine drives.

Norbert C. Cheung (S'85–M'91–SM'05) received the B.Sc. degree from the University of London, London, U.K., in 1981, the M.Sc. degree from the University of Hong Kong, Pok Fu Lam, Hong Kong, in 1987, and the Ph.D. degree from the University of New South Wales, Sydney, Australia, in 1995.

He is currently with the Department of Electrical Engineering, Hong Kong Polytechnic University, Kowloon, Hong Kong. His research interests are motion control, actuators design, power electronic drives, and measurement systems.

Wai-Chuen Gan (S'94–M'02–SM'07) received the B.Eng. degree (with first-class honors and the academic achievement award) in electronic engineering and the M.Phil. and Ph.D. degrees in electrical and electronic engineering from Hong Kong University of Science and Technology, Kowloon, Hong Kong, in 1995, 1997, and 2001, respectively.

From 1997 to 1999, he was a Motion Control Application Engineer with ASM Assembly Automation Hong Kong Ltd., Kwai Chung, Hong Kong. He rejoined the same company in 2002 and is currently a Section Manager in the R&D Motion Group. His current research interests include robust control of ac machines, power electronics, and design and control of linear switched reluctance motors and linear permanent magnet motors.

Dr. Gan is a member of the Hong Kong Institution of Engineers.

Zhen Gang Sun (S'08) received the B.Sc. and M.Sc. degrees from South China University of Technology, Guangzhou, China, in 2000 and 2003, respectively. He is currently working toward the Ph.D. degree in the Department of Electrical Engineering, The Hong Kong Polytechnic University, Kowloon, Hong Kong.

His main research interests include motion control and magnetic levitation machines.